Nuclear Physics B229 (1983) 115–141

ZWEIG-FORBIDDEN RADIATIVE ORTHOQUARKONIUM DECAYS IN PERTURBATIVE QCD

Jürgen G. KÖRNER

Johannes Gutenberg-Universität Mainz, West Germany

J.H. KÜHN

Institut für Theoretische Physik, TH Aachen, West Germany

M. KRAMMER and Heinz SCHNEIDER

Deutches Elektronen-Synchrotron DESY, Hamburg, West Germany

Received 11 January 1983
(Revised 27 May 1983)

We calculate helicity amplitudes and decay rates for Zweig-forbidden radiative decays of a $^3S_1(Q\bar{Q})$ bound state into $^1S_0(q\bar{q})$ and $^3P_J(q\bar{q})$ states in lowest-order QCD. We employ a new technique of scalarizing loop integrals by using covariant helicity projectors. Thereby we are able to integrate analytically all occurring loop integrals.

When applied to J/ψ decays our results are in reasonable agreement with present experimental results. ψ' decays will provide a further test of the model. Transitions from bottonium to charmonium are most interesting since there all dynamical assumptions are well satisfied. Unfortunately the transition rates are very small.

1. Introduction

Radiative decays of J/ψ into lighter mesons have aroused considerable interest from the very beginning. Soon it became clear that in most of these decays the photon couples directly to the heavy quark as suggested by QCD. To estimate the total rate and the inclusive photon spectrum, the decay into a photon and a pair of gluons was calculated [1]. To predict exclusive channels, this approach was pushed even further and duality was assumed between single mesons and the gluon pair projected onto the corresponding spin-parity configurations [2].

Here we want to advocate a completely different approach. We take the diagrams of perturbative QCD (fig. 1) seriously and assume that light and heavy mesons can be considered as dominantly quark–antiquark systems. In addition we use the non-relativistic quark model in the weak-binding approximation for heavy and light bound states. Within this framework we shall calculate helicity amplitudes and decay rates for $^3S_1 \to \gamma + {}^1S_0$ and $^3S_1 \to \gamma + {}^3P_J$ $(J = 0, 1, 2)$ in closed form in terms of logarithms and Spence functions. Thus our model allows us to determine exclusive quarkonium decays completely within perturbative QCD; in particular we do not have to resort to intrinsic non-perturbative quantities like fragmentation functions.

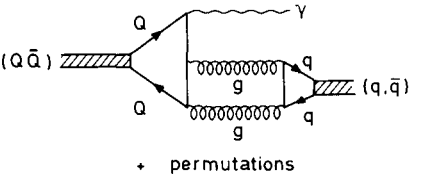

Fig. 1. Lowest-order QCD diagram for the decay of a 1^{--} bound state into a photon and a lighter meson.

Let us stress at this point, that our only input, the wave functions and their derivatives at the origin for S- and P-waves respectively, can be deduced from $J/\psi \to e^+e^-$, $\eta' \to \gamma\gamma$ and $f \to \gamma\gamma$ decays, such that no free parameter enters our calculation.

Decays of the type $(b\bar{b}) \to \gamma + (c\bar{c})$ are of course most attractive from the theoretical viewpoint since in this case our assumptions are well founded. Unfortunately, the corresponding rates are very small. On the other hand our approximations may be disputed for light mesons. Nevertheless, if we compare our calculations with the experimental results, we find consistency and surprising agreement in most if not all cases. In addition we predict the rates of the Zweig-forbidden radiative ψ' and Υ decays which will be measured in the future.

Apart from this practical success our model is an interesting theoretical laboratory and the predictions can be contrasted with those of models based on gluon–meson duality [2]. Indeed some of the most striking consequences of the latter are absent in our model which is in accord with the data. Since contributions from highly virtual gluons play an important role in our approach, there is no drastic suppression of spin-0 versus spin-2 mesons as predicted by duality [2]. This implies in addition, that η' production from Υ is not as much suppressed as most other models [3, 2, 15] would predict. Furthermore the decay into $\gamma + 1^{++}$ mesons is somewhat smaller than $\gamma + 2^{++}$, but not as drastically suppressed as expected, if only quasi-real gluons would contribute.

Some of the results which will be discussed in the following have been obtained previously. The relative magnitude of the absorptive contribution to the three helicity amplitudes in the case of $1^{--} \to \gamma + 2^{++}$ has been obtained by Krammer [3]. The analytic result for $1^{--} \to \gamma + 0^{-+}$ (absorptive and dispersive contribution) has been given by Guberina and Kühn [4]. Here we shall give a more compact form and applications to a large variety of $1^{--} \to \gamma + 0^{-+}$ decays*. A brief discussion of the results for $1^{--} \to \gamma + 1^{++}$ has been given by Körner and Krammer [7] and for $1^{--} \to \gamma + 2^{++}$ by Körner, Kühn and Schneider [8]**. Here we want to present the method of our calculation, the new result for $1^{--} \to \gamma + 0^{++}$ and applications to a large number of decays.

* An earlier numerical evaluation of the same process by Munehisa [5] differs drastically from our result in normalization and mass dependence. A later numerical evaluation by Devoto and Repko [6] differs by a factor $(1 + m^2/M^2)M/2m$.

** Numerical work on P-wave decays has been reported in an unpublished preprint by Nishimura [9].

The outline of our paper is as follows.

In sect. 2 we show how to obtain a set of independent scalar helicity amplitudes and how to decompose the resulting five-point loop functions into a sum of three-point functions, which can be integrated in a straightforward manner. In sect. 3 we first give angular distributions for the decay chain $e^+e^- \to J/\psi \to \gamma + {}^3P_J \to \gamma + M_1M_2$ where we allow for arbitrary complex helicity amplitudes. Then we predict the relative magnitude of the various helicity amplitudes and discuss their physical relevance. In sect. 4 we calculate the rates of radiative J/ψ, ψ' and Y decays in terms of $\Gamma(J/\psi \to e^+e^-)$, $\Gamma(\eta' \to \gamma\gamma)$ and $\Gamma(f \to \gamma\gamma)$ and compare with presently measured branching ratios. Sect. 5 contains our conclusions. In appendix A we present covariant helicity projectors for the different spin cases. In appendix B we discuss the connection between helicity and multipole amplitudes. In appendix C we describe our method to decompose the five-point loop functions into three-point functions and list the basic integrals.

2. Evaluation of Zweig-forbidden radiative transitions

To evaluate quarkonium production and decays, it is useful to apply the bound-state formalism as described e.g. in ref. [10]. It allows us a straightforward evaluation of the covariant amplitudes which describe the effective couplings between the ${}^3S_1$, a real photon and two virtual gluons on the one side and between the ${}^3P_J$ or ${}^1S_0$ and two virtual gluons on the other side. Once these are calculated one just has to multiply the two amplitudes, insert the gluon propagators and perform the loop integrations. It is thus possible to use the non-relativistic model even in a situation where two such systems are highly relativistic with respect to each other.

The amplitude for the coupling of a ${}^3S_1$ vector state with polarization E, momentum K and mass M to a photon (ε, k) and two virtual gluons $(\varepsilon_{1,2}, k_{1,2})$ reads [3] (fig. 2a)

$$A^{V}_{\alpha\nu\nu_1\nu_2} E^{\alpha} \varepsilon^{*\mu} \varepsilon_1^{*\nu_1} \varepsilon_2^{*\nu_2} = 8i \frac{R_V(0)}{\sqrt{4\pi M^3}} \frac{M^2}{(k_1+k_2)\cdot k(k+k_1)\cdot k_2(k+k_2)\cdot k_1} a_V$$

$$\begin{aligned} a_V = {} & \{\varepsilon_1^* \cdot \varepsilon_2^* [-k_1 \cdot k\varepsilon^* \cdot k_2 E \cdot k_1 - k_2 \cdot k\varepsilon^* \cdot k_1 E \cdot k_2 - k_1 \cdot k k_2 \cdot kE \cdot \varepsilon^*] \\ & + E \cdot \varepsilon^* [k_1 \cdot k\varepsilon_1^* \cdot k_2 \varepsilon_2^* \cdot k + k_2 \cdot k\varepsilon_2^* \cdot k_1 \varepsilon_1^* \cdot k - k_1 \cdot k_2 \varepsilon_1^* \cdot k\varepsilon_2^* \cdot k]\} \\ & + \{\varepsilon_1, k_1 \leftrightarrow \varepsilon, k\} + \{\varepsilon_2, k_2 \leftrightarrow \varepsilon, k\}, \end{aligned} \tag{2.1}$$

and reduces to the well-known Ore–Powell amplitude for $k^2 = k_1^2 = k_2^2 = 0$. Also the couplings of two gluons to the pseudoscalar ${}^1S_0$ and to three ${}^3P_J$ states (fig. 2b) have been obtained previously [4, 10]

$$A^{PS}_{\nu_1\nu_2} \varepsilon_1^{\nu_1} \varepsilon_2^{\nu_2} = -4 \frac{R_{PS}(0)}{\sqrt{4\pi m}} \frac{1}{k_1 \cdot k_2} \in (\varepsilon_1, \varepsilon_2, k_1, k_2). \tag{2.2}$$

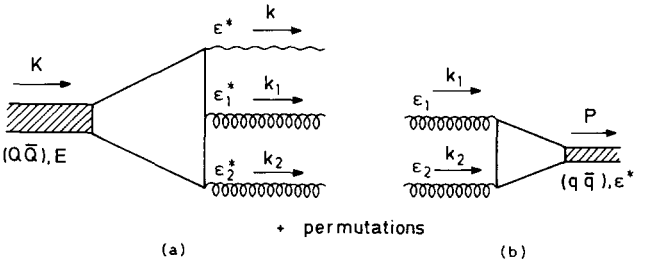

Fig. 2. Lowest-order QCD diagrams for the coupling of a 1^{--} bound state to a photon and two gluons (a) and for the coupling of two gluons to a bound state of positive charge conjugation (b).

$$A^J_{\nu_1\nu_2}\varepsilon_1^{\nu_1}\varepsilon_2^{\nu_2} = 8\sqrt{2}\sqrt{\frac{3}{4\pi m^3}}R'_{\mathrm{P}}(0)\left(\frac{1}{k_1\cdot k_2}\right)^2 a_J$$

$$a_0 = \sqrt{\tfrac{1}{6}}\{[\varepsilon_1\cdot\varepsilon_2 k_1\cdot k_2 - \varepsilon_1\cdot k_2\varepsilon_2\cdot k_1][m^2+k_1\cdot k_2]$$
$$+\varepsilon_1\cdot k_2\varepsilon_2\cdot k_2 k_1^2+\varepsilon_1\cdot k_1\varepsilon_2\cdot k_1 k_2^2-\varepsilon_1\cdot\varepsilon_2 k_1^2k_2^2-\varepsilon_1\cdot k_1\varepsilon_2\cdot k_2 k_1\cdot k_2\},$$

$$a_1 = \tfrac{1}{2}m\{(k_1^2\in(e^*,\varepsilon_1,\varepsilon_2,k_2)+\varepsilon_1\cdot k_1\in(e^*,\varepsilon_2,k_1,k_2))$$
$$+(1\leftrightarrow 2)\},$$

$$a_2 = \sqrt{\tfrac{1}{2}}\,m^2\{k_1\cdot k_2\varepsilon_{1a}\varepsilon_{2b}+k_{2a}k_{1b}\varepsilon_1\cdot\varepsilon_2-k_{1a}\varepsilon_{2b}\varepsilon_1\cdot k_2-k_{2a}\varepsilon_{1b}\varepsilon_2\cdot k_1\}e^{*ab}.$$

(2.3)

Here e_a (e_{ab}) denote the polarization vector (tensor) for the spin-1 (2) bound state of mass m and momentum P. $R_{\mathrm{V}}(0)$ and $R_{\mathrm{PS}}(0)$ denote the radial wave functions of the S-waves, $R'_{\mathrm{P}}(0)$ the derivative of the radial P-wave function at the origin.

In order to illustrate our method of loop integration, we shall discuss the necessary steps in detail for the case $1^{--}\to\gamma+0^{-+}$. We have to evaluate

$$T^{\mathrm{PS}}_{\alpha\nu}E^{\alpha}\varepsilon^{*\nu} = \frac{1}{2}\int\frac{\mathrm{d}^4k_1}{(2\pi)^4}A^{\mathrm{V}}_{\alpha\nu\nu_1\nu_2}E^{\alpha}\varepsilon^{*\nu}A^{\mathrm{PS}\nu_1\nu_2}\frac{i}{k_1^2+i\varepsilon}\frac{i}{k_2^2+i\varepsilon}. \tag{2.4}$$

The factor $\frac{1}{2}$ takes into account that both amplitudes have already been symmetrized with respect to the two gluons. Coupling constants and color factors have been suppressed. The coupling of a vector to a photon and a pseudoscalar is described by one independent helicity amplitude H^{PS}. Instead of evaluating $T^{\mathrm{PS}}_{\alpha\nu}$ (a tensor of rank two) it is therefore sufficient to calculate the scalar H^{PS}, which is obtained from $T^{\mathrm{PS}}_{\alpha\nu}$ with the help of a helicity projector (appendix A). For the pseudoscalar case it is particularly simple

$$H^{\mathrm{PS}} = T^{\mathrm{PS}}_{\alpha\nu}\mathbb{P}^{\mathrm{PS}\alpha\nu}, \tag{2.5}$$

where

$$\mathbb{P}^{\mathrm{PS}}_{\alpha\nu} = -\frac{i}{2P\cdot k}\varepsilon_{\alpha\nu\rho\lambda}P^{\rho}k^{\lambda},$$
$$\mathbb{P}^{\mathrm{PS}}_{\alpha\nu}\mathbb{P}^{*\mathrm{PS}\alpha\nu} = \tfrac{1}{2}, \tag{2.6}$$

and of course $T^{PS}_{\alpha\nu}$ can be reconstructed from H^{PS}

$$T^{PS}_{\alpha\nu} = -2H^{PS}\mathbb{P}^{PS}_{\alpha\nu}. \tag{2.7}$$

After some algebra one finds

$$H^{PS} = \tfrac{1}{2}8i\frac{R_V(0)}{\sqrt{4\pi M^3}}\frac{4R_{PS}(0)}{\sqrt{4\pi m}}\frac{1}{(2\pi)^4}\frac{\pi^2}{i}i\hat{H}^{PS},$$

$$\hat{H}^{PS} = -\frac{M^2}{2P\cdot k}\frac{i}{\pi^2}\int\frac{1}{16}d^4q\frac{(P\cdot k)q^2-(q\cdot k)(q\cdot P)}{(k_1+k)\cdot k_2(k_2+k)\cdot k_1(k_1^2+i\varepsilon)(k_2^2+i\varepsilon)},$$

$$q = k_1 - k_2, \qquad P = k_1 + k_2. \tag{2.8}$$

Note, that the $k_1\cdot k_2$ denominator has cancelled. In principle this leads to a three-Feynman-parameter integral. With the help of the algebraic identity

$$(P\cdot k)q^2-(q\cdot k)(q\cdot P) = \frac{2P\cdot k}{M^2+m^2}[m^2((k_1+k)\cdot k_2+(k_2+k)\cdot k_1)+M^2(k_1^2+k_2^2)] - q\cdot k(k_1^2-k_2^2), \tag{2.9}$$

the integrand can be decomposed into a sum of three-point functions which are listed in appendix C.

$$\hat{H}^{PS} = \frac{4}{x}\left[\mathscr{L}_2(1-2x)-\mathscr{L}_2(1)-\frac{x}{1-2x}\ln(2x) - \frac{1-x}{2-x}(2\mathscr{L}_2(1-x)-2\mathscr{L}_2(1)+\tfrac{1}{2}\ln^2(1-x))\right] + i\pi 4\frac{1-x}{(2-x)x}\ln(1-x),$$

$$x = 1-m^2/M^2. \tag{2.10}$$

The real and imaginary parts of $\hat{H}^{PS}$ are shown in fig. 3. The behaviour of $\hat{H}^{PS}$ in the limit of small and large x is given by

$$\hat{H}^{PS}(x) \xrightarrow[x\to 0]{} 4[\ln 2-1]-2i\pi,$$

$$\hat{H}^{PS}(x) \xrightarrow[x\to 1]{} 4[\ln 2-\tfrac{1}{4}\pi^2-\tfrac{1}{2}(1-x)\ln^2(1-x)]+4i\pi(1-x)\ln(1-x). \tag{2.11}$$

For $x\to 1$ $(m^2/M^2\to 0)$ the amplitude is dominated by the dispersive part, i.e. the contribution of off-shell gluons. In refs. [2, 3] it was pointed out that the production of (on-shell) gluons in the partial wave 0^{-+} is suppressed by a factor m^2/M^2 relative to the 2^{++} contribution due to the special form of the Ore–Powell matrix element

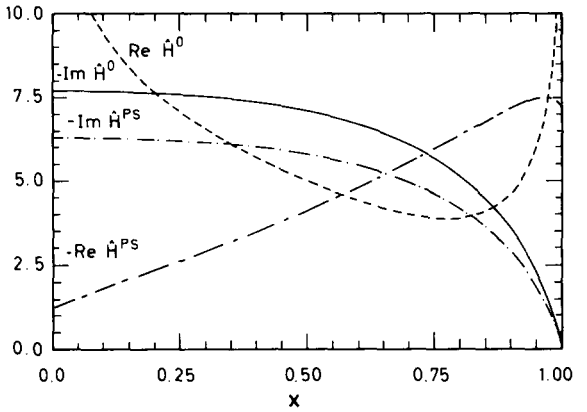

Fig. 3. Real and imaginary parts of the dimensionless helicity amplitudes $\hat{H}$ for the two spin-zero cases 0^{-+} and 0^{++} as function of $x = 1 - m^2/M^2$.

which explains the smallness of the absorptive part. For off-shell gluons this suppression is no longer operative [4]. At this point we want to stress that the mass dependence of the rate differs from that of Novikov et al. [15] by an additional factor $(M/m)^4$. Thus we expect that our contribution will dominate for heavy quarkonia.

In the limit $m^2/M^2 \to 0$ the light quark mass can be neglected and the methods used to study hadronic form factors at large Q^2 [24] are applicable. For arbitrary light meson wave functions the contributions from light-like distances dominate and the general distribution amplitude on the lightcone is related to our non-relativistic wave function by

$$\varphi_{NR}(u) = \sqrt{3} \cdot 4 \frac{R_{PS}}{\sqrt{4\pi m}} \delta(u) ,$$

where $\frac{1}{2}(1 \pm u)$ denotes the momentum fraction of quark and antiquark. In this paper we shall calculate the rate for the arbitrary mass ratio m/M, since in general the mass of the light meson cannot be neglected compared with M. (This holds in particular for the P-states f and f'). In order to keep the problem tractable we make use of the non-relativistic approximation. Results in the limit $m^2/M^2 \to 0$ and $\varphi(u)$ arbitrary, which may be relevant for light pseudoscalars, will be published elsewhere [25]. The scaling law for the rate as a function of M in the limit $m^2/M^2 \to 0$ coincides with the predictions of ref. [24] based on constituent counting rules and helicity considerations. However, note that the leading contribution from a 0^{+-}-two-gluon final state has a different scaling law. To obtain the decay rate, we multiply the amplitude with the appropriate coupling constants, the quark charge Q and a color

factor $\frac{2}{3}$:

$$\Gamma(^3S_1 \to {}^1S_0 + \gamma) = \tfrac{1}{6}(\tfrac{2}{3})^2 \alpha_s^4 \alpha Q^2 \frac{1}{M^3} \left(\frac{4R_V(0)}{\sqrt{4\pi M}}\right)^2 \left(\frac{4R_{PS}(0)}{\sqrt{4\pi m}}\right)^2 x|\hat{H}^{PS}(x)|^2$$

$$x|\hat{H}^{PS}|^2 \text{ is shown in fig. 6.} \tag{2.12}$$

Let us mention that the phase of $\hat{H}^{PS}$ can be determined in principle, if the S-dependent interference between resonant $\eta'\gamma$ production and the continuum contribution could be measured [4]. In our model the latter is estimated

$$\frac{\sigma(e^+e^- \to \gamma^* \to {}^1S_0\gamma)}{\sigma(e^+e^- \to \gamma^* \to \mu^+\mu^-)} = \frac{8}{\alpha}\frac{m}{s}\left(1 - \frac{m^2}{s}\right)^{1/2} \Gamma({}^1S_0 \to \gamma\gamma), \tag{2.13}$$

which amounts to $\sim 0.5 \cdot 10^{-3}$ for $\eta'\gamma$ production just below the J/ψ resonance. With present luminosities the prospects for this measurement are not promising. Similar considerations apply to P-wave production discussed later on. Due to the smallness of the corresponding interference effects we shall not pursue this subject further.

The calculation of $\Gamma(^3S_1 \to {}^3P_J + \gamma)$, which is the main subject of this paper, has indeed many similarities with the previous one. We use the analogue of eq. (2.4) to obtain the tensors of rank 2, 3 and 4, which describe the production of 0^{++}, 1^{++} and 2^{++} mesons. With the help of the helicity projectors described in appendix A we find the independent helicity amplitudes. In the spin-0 case for example there is again only one projector $\mathbb{P}^0$ (A.3) and one independent amplitude $H^{(0)}$. After some algebra we find

$$H^{(0)} \equiv \frac{1}{2}\int \frac{d^4k_1}{(2\pi)^4} A^V * A^0 * \mathbb{P}^0 \frac{i}{k_1^2 + i\varepsilon}\frac{i}{k_2^2 + i\varepsilon}$$

$$= -i\frac{4R_V(0)}{\sqrt{4\pi M^3}}\sqrt{\frac{3}{4\pi m^3}}\, 8\sqrt{2}\, R'_P(0)\frac{1}{(2\pi)^4}\frac{\pi^2}{i}\hat{H}^0, \tag{2.14}$$

where

$$\hat{H}^{(0)} = \frac{i}{\pi^2}\int \tfrac{1}{16} d^4q \frac{f(q,k,P)}{(k_1+k)\cdot k_2(k_2+k)\cdot k_1(k_1^2+i\varepsilon)(k_2^2+i\varepsilon)}, \tag{2.15}$$

$$q = k_1 - k_2, \qquad P = k_1 + k_2,$$

and f denotes a scalar even polynomial in q. In contrast to the pseudoscalar case now the numerator f depends on q up to terms of fourth order, the denominator (k_1k_2) is no longer cancelled and one is led to integrals with up to four Feynman parameters. It is, however, possible to decompose the integrand into a sum of three-point functions (appendix C) which can be solved in a straightforward manner in terms of logarithms and Spence functions. The resulting integrals are listed in

appendix C. For $\hat{H}^{(0)}$ we finally obtain

$$\hat{H}^{(0)}(x)=\sqrt{\frac{2}{3}}\left[\frac{2-3x}{x^2}+\left(10\frac{1-x}{x^3}+4\frac{1-2x}{x^2}\ln 2\right)\ln(1-x)\right.$$
$$-3\frac{1-x}{x(2-x)}\ln^2(1-x)+\left(\frac{8}{x^2}+2\frac{1-x}{x(1-2x)}\right)\ln(2x)$$
$$+\frac{8-6x+x^2-6x^3}{x^3(2-x)}\mathscr{L}_2(1)-\frac{4-5x+2x^2}{x^3}\mathscr{L}_2(1-2x)$$
$$\left.-4\frac{2-2x-x^2}{x^2(2-x)}\mathscr{L}_2(1-x)+i\pi 6\frac{1-x}{x(2-x)}\ln(1-x)\right]. \qquad (2.16)$$

The behaviour of $\hat{H}^{(0)}$ in the limits of small and large x is given by

$$\hat{H}^{(0)}(x)\xrightarrow[x\to 0]{}\sqrt{\tfrac{2}{3}}\left[\tfrac{29}{9}+\tfrac{10}{3}\ln 2-\tfrac{8}{3}\ln x-3i\pi\right],$$

$$\hat{H}^{(0)}(x)\xrightarrow[x\to 1]{}\sqrt{\tfrac{2}{3}}\left[8\ln 2-1-\tfrac{5}{12}\pi^2-4\ln 2\ln(1-x)+i\pi 6(1-x)\ln(1-x)\right]. \qquad (2.17)$$

Due to the P-wave denominator $(k_1k_2)^{-2}$ the integrals diverge logarithmically in both limits, in contrast to the pseudoscalar case. The real part dominates again in the limit $m^2/M^2\to 0$ $(x\to 1)$ since the Ore–Powell amplitude supresses also the production of real gluons in the 0^{++} configuration [2]. In fig. 3 we plot the real and imaginary parts of $\hat{H}^{(0)}$.

For 1^{++} production there are two independent amplitudes $H_0^{(1)}$ and $H_1^{(1)}$. We multiply A^{V} and A^1 from eq. (2.1) and (2.2), project onto the proper helicity basis with the help of the two projectors $\mathbb{P}_i^1$ $(i=0,1)$ defined in appendix A and obtain two integrands of a similar structure as in the 0^{++} case. They are decomposed into a sum of three-point functions and integrated with the same techniques as before (appendix C). In this case one gluon propagator is immediately cancelled due to the $k_{1,2}^2$ factor in eq. (2.3) dictated by "Yang's theorem". One finds (see also ref. [7])

$$\hat{H}_i^{(1)}=i\frac{4R_{\mathrm{V}}(0)}{\sqrt{4\pi M^3}}8\sqrt{2}\sqrt{\frac{3}{4\pi m^3}}R'_{\mathrm{P}}(0)\frac{1}{(2\pi)^4}\frac{\pi^2}{i}i\hat{H}_i^{(1)},$$

$$\hat{H}_1^{(1)}=4\frac{\sqrt{1-x}}{x^2}\left[\frac{1}{x}(\mathscr{L}_2(1)-\mathscr{L}_2(1-2x))-x-2x(\mathscr{L}_2(1-x)-\mathscr{L}_2(1-2x)\right.$$
$$\left.-\ln 2\ln(1-x))+\frac{2-x-2x^2}{x}\ln(1-x)+2(1+x)\ln(2x)\right],$$

$$\hat{H}_0^{(1)} = 4\frac{1}{x^2}\left[\frac{1}{x}(\mathscr{L}_2(1)-\mathscr{L}_2(1-2x))-6(1-x)(\mathscr{L}_2(1-x)-\mathscr{L}_2(1-2x)\right.$$
$$\left.-\ln 2\ln(1-x))+\frac{2}{x}(1-x)(1-2x)\ln(1-x)+\frac{2-8x+7x^2}{1-2x}\ln(2x)\right], \tag{2.18}$$

with the limiting behaviour.

$$\hat{H}_0^{(1)} \xrightarrow[x\to 1]{} \pi^2-4\ln 2\,,$$

$$H_1^{(1)} \xrightarrow[x\to 1]{} 4\sqrt{1-x}\,[-1+\tfrac{1}{12}\pi^2+4\ln 2-\ln(1-x)+2\ln 2\ln(1-x)]\,, \tag{2.19}$$

$$\hat{H}_0^{(1)} \xrightarrow[x\to 0]{} \tfrac{26}{9}-\tfrac{8}{3}\ln(2x)\,, \tag{2.20}$$

$$\hat{H}_1^{(1)} \xrightarrow[x\to 0]{} \tfrac{26}{9}-\tfrac{8}{3}\ln(2x)\,. \tag{2.21}$$

The longitudinal amplitude dominates for $m \ll M$: $H_1/H_0 = O((m/M)\ln(m/M))$ as expected. In the nearly equal mass case the electric dipole transition dominates: $H_1/H_0 \to_{x\to 0} 1$ (see appendix B), which provides an additional check on our calculation. The absorptive contribution vanishes identically since 1^{++} does not couple to real gluons. The dispersive part is shown in fig. 4. The overall magnitude of the amplitudes for scalar, axialvector and, as we shall see, tensor mesons is roughly the same and our model does not confirm the enhancement of 2^{++} versus 0^{++} and 1^{++}, which would be natural if virtual gluons did not contribute [2].

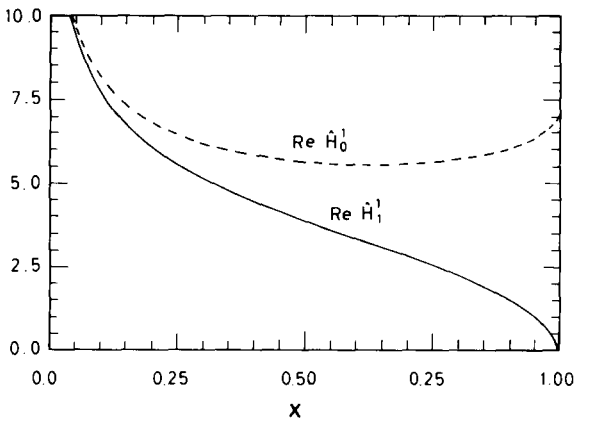

Fig. 4. Dispersive contribution to the two dimensionless helicity amplitudes $\hat{H}_0^{(1)}$ and $\hat{H}_1^{(1)}$ in the 1^{++} case as function of x. The absorbtive contribution vanishes.

For the spin-two case we proceed as before. The three helicity projectors $\mathbb{P}_i^2$ ($i=0,1,2$) are given in appendix A. One finds [8]*

$$H_i^{(2)} = i\frac{4R_V(0)}{\sqrt{4\pi M^3}}8\sqrt{2}\sqrt{\frac{3}{4\pi m^3}}R_P'(0)\frac{1}{(2\pi)^4}\frac{\pi^2}{i}\hat{H}_i^{(2)},$$

$$\hat{H}_0^{(2)} = \frac{2\sqrt{3}}{x^3}\Bigg[(6-5x)x+\frac{2}{3}\frac{6-19x+18x^2}{x}(1-x)\ln(1-x)$$

$$-\frac{1}{3}\frac{10-12x+5x^2}{2-x}(\mathscr{L}_2(1)-\mathscr{L}_2(1-2x))+\frac{2}{3}\frac{6-38x+71x^2-37x^3}{1-2x}\ln(2x)$$

$$-8\frac{(1-x)^2}{x^2(2-x)}(\mathscr{L}_2(1-2x)-2\mathscr{L}_2(1-x)-\tfrac{1}{2}\ln^2(1-x)+\mathscr{L}_2(1)+i\pi\ln(1-x))$$

$$+\frac{4}{3}\frac{6-6x-x^2}{x}(\ln 2-\tfrac{1}{2}i\pi)-\tfrac{4}{3}(12-26x+13x^2)$$

$$\times(\mathscr{L}_2(1-x)-\mathscr{L}_2(1-2x)-\ln 2\ln(1-x))\Bigg],$$

$$\hat{H}_1^{(2)} = 2\frac{\sqrt{1-x}}{x^3}\Bigg[-\tfrac{1}{3}(38-9x)x-\frac{2}{x}(4-13x+16x^2-4x^3)\ln(1-x)$$

$$+2\frac{x(1-x)}{2-x}(\mathscr{L}_2(1)-\mathscr{L}_2(1-2x))-\frac{4}{1-2x}(2-11x+16x^2-4x^3)\ln(2x)$$

$$+8\frac{(1-x)(2-2x+x^2)}{x^2(2-x)}(\mathscr{L}_2(1-2x)-2\mathscr{L}_2(1-x)-\tfrac{1}{2}\ln^2(1-x)+\mathscr{L}_2(1)$$

$$+i\pi\ln(1-x))$$

$$-\frac{16}{3}\frac{3-3x+x^2}{x}(\ln 2-\tfrac{1}{2}i\pi)+4(8-12x+3x^2)$$

$$\times(\mathscr{L}_2(1-x)-\mathscr{L}_2(1-2x)-\ln 2\ln(1-x))\Bigg],$$

$$\hat{H}_2^{(2)} = \sqrt{2}\frac{1-x}{x^3}\Bigg[\tfrac{16}{3}x+\frac{4}{x}(1-6x+6x^2)\ln(1-x)$$

$$-\frac{2}{2-x}(5-6x+2x^2)(\mathscr{L}_2(1)-\mathscr{L}_2(1-2x))+4(1-6x)\ln(2x)$$

$$-4\frac{2-4x+6x^2-4x^3+x^4}{x^2(2-x)}(\mathscr{L}_2(1-2x)-2\mathscr{L}_2(1-x)-\tfrac{1}{2}\ln^2(1-x)+\mathscr{L}_2(1)$$

$$+i\pi\ln(1-x))$$

* Our normalization convention differs from that of ref. [8] by a factor $1/2\sqrt{2}$.

$$+\frac{4}{3}\frac{6-6x+11x^2}{x}(\ln 2-\tfrac{1}{2}i\pi)-16(1-x)$$
$$\times(\mathscr{L}_2(1-x)-\mathscr{L}_2(1-2x)-\ln 2\ln(1-x))\Big]. \tag{2.22}$$

The relative magnitude of the absorbtive parts Im $\hat{H}_i^{(2)}$ agrees with earlier calculations [3]. In the limit $x\to 1$ one finds

$$\hat{H}_0^{(2)} \xrightarrow[x\to 1]{} \frac{4}{\sqrt{3}}[-2\ln 2\ln(1-x)-4\ln 2+\tfrac{3}{4}-\tfrac{5}{24}\pi^2+i\pi],$$

$$\hat{H}_1^{(2)} \xrightarrow[x\to 1]{} 4\sqrt{1-x}\,[2\ln 2\ln(1-x)-3\ln(1-x)+\tfrac{10}{3}\ln 2-\tfrac{29}{6}-\tfrac{1}{6}\pi^2+\tfrac{4}{3}i\pi].$$

$$\hat{H}_2^{(2)} \xrightarrow[x\to 1]{} -2\sqrt{2}\,(1-x)[-\ln^2(1-x)-2\ln(1-x)+\tfrac{8}{3}\ln 2-\tfrac{8}{3}+\tfrac{5}{12}\pi^2$$
$$+2\pi i(\ln(1-x)+\tfrac{11}{6})]. \tag{2.23}$$

Up to logarithmic factors the three amplitudes behave as $(1-x)^0:(1-x)^{1/2}:(1-x)^1$. The origin of this relative $(1-x)$ power is the mass dependent normalization factor m^{-1} of the helicity-zero spin-1 states that are used to construct the spin-2 f-meson*. For $x\to 0$ on the other hand (soft photon limit) the electric dipole transition dominates

$$\hat{H}_0^{(2)} \sim \sqrt{\tfrac{1}{3}}\,\hat{H}_1^{(2)} \sim \sqrt{\tfrac{1}{6}}\,\hat{H}_2^{(2)} \sim \frac{4}{5\sqrt{3}}(\tfrac{10}{3}\ln x+\tfrac{4}{3}\ln 2-\tfrac{16}{9}+i\pi). \tag{2.24}$$

As can be seen from eqs. (2.4) and (2.5), the amplitudes are dominantly real both for $x\to 0$ and $x\to 1$.

Fig. 5 shows the three $H_i^{(2)}$ in an Argand plot. The individual phases decrease monotonically from 180° at $x=0$ to 0° at $x=1$. It is quite remarkable that the

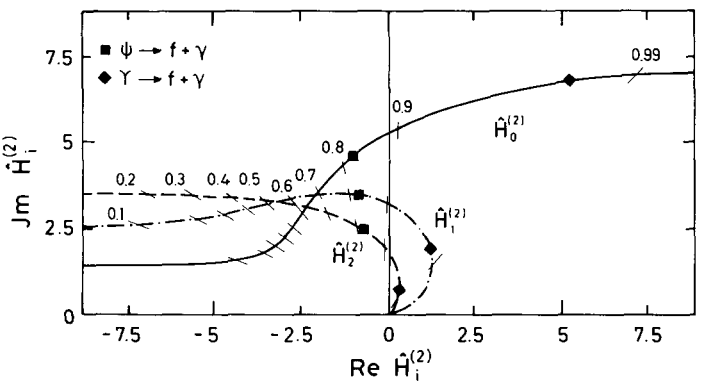

Fig. 5. Argand plot of the dimensionless helicity amplitudes $\hat{H}_i^{(2)}$ as functions of x.

* This result is consistent with ref. [24] which predicts the dominance of the helicity-0 final states in the limit $m^2/M^2\to 0$. For the reaction $J/\psi\to f+\gamma$ however helicity 1 and 2 contributions are still of comparable importance (cf. table 1) and only $\Upsilon\to f+\gamma$ can be treated in this limit. Note, that the naive scaling law for the rate as function of M is modified by a logarithmic factor.

three amplitudes are very close in phase over the whole range $0 \leq x \leq 1$ (for $0 \leq x < 0.6$ their phase difference never exceeds one degree) and thus the original predictions for the relative magnitudes $H_1^{(2)}/H_0^{(2)}$ and $H_2^{(2)}/H_0^{(2)}$ which were only based on the absorptive parts remain practically unchanged.

In order to obtain the decay rate for all three P-states we multiply with the electric- and strong-coupling constants, the quark charge Q and the color factor $(\frac{2}{3})^2$

$$\Gamma(^3S_1 \to {}^3P_J + \gamma) = \frac{1}{6M} \frac{1}{4\pi} \frac{|\boldsymbol{p}_\gamma|}{M} \cdot 2 \sum_i |H_i^J|^2$$

$$= \alpha Q^2 \alpha_s^4 \frac{256}{9\pi^2} \frac{|R_V(0)|^2}{M^4} \frac{|R'_P(0)|^2}{m^3} x \sum_i |\hat{H}_i^J|^2 . \qquad (2.25)$$

The sum of the squared reduced amplitudes multipled by x is shown in fig. 6 for the three cases. Over a large x range the production rates for all three P states are of comparable magnitude. For $x \to 1$ we find for their relative strengths

$$|\hat{H}^{PS}|^2 \quad : \quad |\hat{H}^{(0)}|^2 \quad : \sum |\hat{H}_i^{(1)}|^2 \; : \quad \sum |\hat{H}_i^{(2)}|^2$$
$$(\tfrac{1}{4}\pi^2 - \ln 2)^2 : \tfrac{3}{4} \ln^2 2 \ln^2 (1-x) : (\tfrac{1}{4}\pi - \ln 2)^2 : \tfrac{4}{3} \ln^2 2 \ln^2 (1-x) , \qquad (2.26)$$

and in the soft photon limit ($x \to 0$)

$$|\hat{H}^{PS}|^2 \; : |\hat{H}^{(0)}|^2 : \sum |\hat{H}_i^{(1)}|^2 : \sum |\hat{H}_i^{(2)}|^2$$
$$\xrightarrow[x \to 0]{} (\ln 2 - 1)^2 : \tfrac{8}{27} \ln^2 x : 3 \cdot \tfrac{8}{27} \ln^2 x : 5 \cdot \tfrac{8}{27} \ln^2 x . \qquad (2.27)$$

Note that, in this limit, the P-wave states are produced with weights $2J+1$.

3. Angular distributions

Although the absolute rates depend crucially on our input values for α_s and $R(0)$, the relative magnitudes of the various helicity amplitudes are predicted independent of any adjustable parameter and depend on the mass ratio m^2/M^2 only. They can be determined experimentally from an analysis of the angular distributions in the

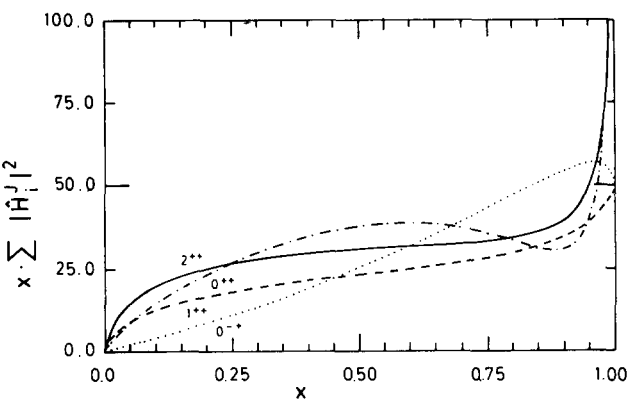

Fig. 6. Summed squares of the reduced amplitudes $x \sum |\hat{H}_i^J|^2$ for the four cases 0^{-+}, 0^{++}, 1^{++}, 2^{++}.

decay chain $^3S_1 \to \gamma + {}^3P_J(\to M_1 M_2)$. For decays into spin-zero mesons the form of the amplitude for the decay $^3P_J \to M_1 M_2$ is uniquely fixed.

$$A_{J=0} = \text{const}, \qquad A_{J=1} = \varepsilon p, \qquad A_{J=2} = \varepsilon_{\mu\nu} p^\mu p^\nu,$$
$$p \equiv p_{M_1} - p_{M_2}. \tag{3.1}$$

For $J=0$ the angular distribution of M_1 and M_2 in their c.m. frame is of course isotropic. Note that for $J=1$ the mesons M_1 and M_2 have to have opposite parities. For $J=1(2)$ we find the 2 (4) parameter angular distributions

$J=2$:

$$\begin{aligned} dN = \frac{15}{256} \frac{d\cos(\theta_\gamma)\, d\phi_p\, d\cos\theta_p}{\pi(1+|X|^2+|Y|^2)} \\ \times\{(1+\cos^2\theta_\gamma)[2(3\cos^2\theta_p - 1)^2 + 3\sin^4(\theta_p)|Y|^2] \\ + 2\sin^2(\theta_\gamma)[3\sin^2(2\theta_p)|X|^2] \\ + 2\sin^2\theta_\gamma \cos(2\phi_p)[\sqrt{6}\sin^2\theta_p(3\cos^2\theta_p - 1)\,\mathrm{Re}\,Y] \\ + 2\sqrt{2}\sin(2\theta_\gamma)\cos\phi_p[-\tfrac{3}{2}\sin(2\theta_p)\sin^2\theta_p\,\mathrm{Re}(XY^*) \\ + \tfrac{1}{2}\sqrt{6}\sin(2\theta_p)(3\cos^2\theta_p - 1)\,\mathrm{Re}\,X]\}. \end{aligned} \tag{3.2}$$

$J=1$:

$$\begin{aligned} dN = \frac{9}{32} \frac{d\cos\theta_\gamma\, d\phi_p\, d\cos\theta_p}{\pi(1+|X|^2)} \\ \times\{(1+\cos^2\theta_\gamma)\cos^2\theta_p + \sin^2\theta_\gamma \sin^2\theta_p |X|^2 \\ + \tfrac{1}{2}\sin(2\theta_\gamma)\sin(2\theta_p)\cos\phi_p\,\mathrm{Re}\,X\}, \end{aligned} \tag{3.3}$$

where $X \equiv \hat{H}_1/\hat{H}_0$; $Y \equiv \hat{H}_2/\hat{H}_0$. θ_γ is the polar angle between the photon and the e^+ beam axis. θ_p and ϕ_p are the polar and azimuthal angles of M_1 and M_2 in their c.m. frame. The **z**-axis is defined by the flight direction of the M_1M_2 system. The **y**-axis is proportional to $\mathbf{z}\times\mathbf{e}^+$ and $\mathbf{x}=\mathbf{y}\times\mathbf{z}$. ϕ_p is measured in the **xy** plane. For real X and Y this coincides with the one (two) parameter form of Kabir and Hey [10], which was used in the experimental analysis of $J/\psi \to \gamma + f(\to \pi\pi)$. The photon angular distribution is of the form

$$\frac{dN}{d\cos\theta} \propto 1 + \alpha\cos^2\theta,$$
$$\alpha = \begin{cases} 1 & J=0 \\ \dfrac{1-2|X|^2}{1+2|X|^2} & J=1 \\ \dfrac{1-2|X|^2+|Y|^2}{1+2|X|^2+|Y|^2} & J=2. \end{cases} \tag{3.4}$$

TABLE 1

Ratios of helicity amplitudes $X \equiv H_1/H_0$, $Y \equiv H_2/H_0$ (absolute value, phase) for various radiative decays

		J/ψ(3100)	ψ'(3685)	Υ(9460)
D(1285) X		0.36; 0°	0.29; 0°	0.07; 0°
E(1420) X		0.41; 0°	0.32; 0°	0.08; 0°
$\chi_1(3510)$ X				0.31; 0°
f(1270)	X	0.77; 2.0°	0.65; 2.8°	0.27; 5.2°
	Y	0.55; 4.0°	0.42; 6.0°	0.10; 16.2°
f'(1520)	X	0.90; 1.3°	0.77; 2.0°	0.32; 5.0°
	Y	0.72; 2.4°	0.55; 4.0°	0.13; 14.7°
θ(1640)	X	0.96; 1.1°	0.83; 1.7°	0.34; 4.9°
	Y	0.81; 1.8°	0.62; 3.2°	0.15; 14.0°
$\chi_2(3550)$	X			0.70; 2.4°
	Y			0.48; 5.1°

The ratios X and Y are listed in table 1 for the various decay modes of J/ψ, ψ' and Υ.

For J/ψ→γ+f our angular distributions are practically indistinguishable from the previous analysis of Krammer [3], which was based on the absorptive part only. Experimental results have been obtained by PLUTO [12], MARK II [17] and CRYSTAL Ball [17]. The most recent experiment [17] finds $X = 0.88 \pm 0.11$, $Y = 0.04 \pm 0.14$ (only statistical errors are quoted!) assuming, however, in the analysis the ratios X and Y to be real. It remains to be seen, whether a reanalysis of the data using the general distribution (3.2) and including systematic errors reduces the significance of the disagreement between experiment and the model. For $^3S_1 \to \gamma + {}^3P_1$ we find purely real amplitudes, a prediction which should be tested experimentally. We note that the coefficient α of the photon angular distribution in the decay J/ψ→γ+ι(1440) has been measured to be 1.4 ± 0.8 in good agreement with the pseudoscalar assignment 0^{-+}. However, if we would misinterpret ι as a $^3P_1$ state (E(1420)) the model predicts $\alpha = 0.4$, which is disfavored.

4. Application to J/ψ, ψ' and Υ decays

When we apply our model to J/ψ, ψ' and Υ decays, we have to specify α_s and the wave functions at the origin. Decays into light mesons are particularly sensitive

to this input. In the decay $J/\psi \to \gamma + f$ for example it makes a big difference whether we use M_f or M_ψ as the relevant mass scale in the strong-coupling constant α_s*. ** Also the non-relativistic and the zero binding energy approximation may be disputed for light mesons. In our case the wave function at the origin will only serve as a useful parameter which relates the two short-distance processes: two-photon decay of the light mesons and Zweig-forbidden radiative J/ψ decays. We shall now discuss the rates and our input in more detail.

(*a*) *Pseudoscalars.* The rates for $J/\psi \to \gamma + \eta'$ or η and $\Upsilon \to \gamma + \eta_c$ have been discussed previously [4] and we briefly repeat the results for completeness. From $J/\psi \to e^+e^-$ we find $R_V^2(0) = 0.46\,\mathrm{GeV}^3$. For η' the wave function at the origin can be obtained from the two-photon width of 5.0 ± 1.4 keV [13] through the non-relativistic formula

$$\Gamma(^1S_0 \to \gamma\gamma) = 12\alpha^2 \langle Q^2 \rangle^2 R_{PS}^2(0)/m^2 , \tag{4.1}$$

following from eq. (2.2). $\langle Q^2 \rangle$ is related to the SU(3) mixing angle $\theta_{PS} = -11°$ and the charge of singlet and octet combinations

$$\begin{aligned} \langle Q^2 \rangle_{\eta'} &= \langle Q^2 \rangle_1 \cos\theta_{PS} + \langle Q^2 \rangle_8 \sin\theta_{PS} \\ &= \sqrt{\tfrac{1}{3}}\,(\tfrac{4}{9} + \tfrac{1}{9} + \tfrac{1}{9}) \cos\theta_{PS} + \sqrt{\tfrac{1}{6}}\,(\tfrac{4}{9} + \tfrac{1}{9} - \tfrac{2}{9}) \sin\theta_{PS} = 0.35 . \end{aligned} \tag{4.2}$$

The value $R_{PS}^2(0) = 0.059 \pm 0.016\,\mathrm{GeV}^3$ comes surprisingly close to the prediction of the empirical formula for the $^3S_1$ states $R^2(0) = 0.056\,\mathrm{GeV} \cdot M^2$. To obtain the width for $J/\psi \to \gamma + \eta'$ we multiply eq. (2.12) by the SU(3) factor $3\cos^2\theta_{PS}$ and use $\alpha_s = 0.31$ as suggested by the first-order formula for the running coupling constant

$$\alpha_s(m_{\eta'}^2) = \frac{12\pi}{27 \ln (m_{\eta'}^2/\Lambda^2)} , \tag{4.3}$$

with $\Lambda = 100$ MeV. The result $\Gamma(J/\psi \to \gamma + \eta') = 188$ eV is in reasonable agreement with the experimental results of 223 ± 32 eV [18] as listed in table 2.

The estimate for the ratio $\Gamma(J/\psi \to \gamma + \eta)/\Gamma(J/\psi \to \gamma + \eta')$ is rather ambiguous in our model. If we use eq. (4.1) to deduce $R_\eta(0)$ we obtain a disastrously small result ($75\alpha_s^4$ eV). However, if we assume SU(3) invariance for $R_\eta(0)$, i.e. the same value as for η', and $\alpha_s = 0.41$ as suggested by eq. (4.3), we find

$$\frac{\Gamma(J/\psi \to \gamma + \eta')}{\Gamma(J/\psi \to \gamma + \eta)} \approx \left(\frac{\alpha_s(M_{\eta'})}{\alpha_s(M_\eta)}\right)^4 \cot^2\theta_{PS} \frac{M_\eta}{M_{\eta'}} = 5 , \tag{4.4}$$

* α_s (the rate Γ) differs by a factor 1.35 (3.3) for the two choices, if we use eq. (4.3) for α_s and $\Lambda = 100$ MeV.

** If the dominant contribution to the loop integral stems from regions where all intermediate propagators are far off shell, the relevant scale will be M times a finite scale factor s to be determined from higher-order calculations. This is the case in the reaction $^3S_1(Q\bar{Q}) \to \gamma + {}^1S_0(q\bar{q})$ for $m^2/M^2 \to 0$. For $^3S_1(Q\bar{Q}) \to \gamma + {}^3P_2(q\bar{q})$ on the other hand the absorbtive contribution is only logarithmically suppressed and hence the mass of the light meson will also influence the scale for α_s. In practice, however, for radiative J/ψ decays the uncertainty of the scale factor s is equally important and for simplicity we shall use m ($\approx(\frac{1}{4}$ to $\frac{1}{2}) \cdot M_{J/\psi}$)! throughout.

TABLE 2

Measured branching ratios for radiative decays of J/ψ and ψ'

X	Br (J/$\psi\to\gamma$X) · 10^3	Ref.	Br ($\psi'\to\gamma$X)/Br (J/$\psi\to\gamma$X)	Ref.
η	0.85 ± 0.086	[18]	<0.08	[21]
η'	3.55 ± 0.46	[18]	0.06 ± 0.03	[21]
$\iota\cdot$ Br (K$\pi\pi$)	4.0 ± 1.2 Crystal Ball 4.3 ± 1.7 Mark II	[17]	<0.03	[21]
f	1.5 ± 0.35	[18]	<0.2	[20]
f'	<0.4 $0.32\pm0.1\pm0.16$	[19] [20] [22]		
$D\cdot$ Br (K$\bar{\text{K}}\pi$)	<0.7	[19]		
$\theta\cdot$ Br ($\eta\eta$)	0.49 ± 0.24	[17]		

in reasonable agreement with the data. This should be considered as an indication that neither the non-relativistic model nor perturbative QCD are good approximations in this case. Considering these ambiguities we prefer to use the experimental value of 54 eV as input to predict $\psi'\to\gamma+\eta$ and $\Upsilon\to\gamma+\eta$ since we expect the relative rates to be more reliable.

For light pseudoscalars we could alternatively consider the limit $m^2/M^2\to0$ and allow for arbitrary relativistic quark wave functions $\varphi(u)$. This approach which allows us to normalize the decay rate with respect to $\langle0|\partial A|\text{Ps}\rangle$ will be treated elsewhere [25].

It is an interesting problem whether $\iota(1440)$ can be accommodated in our model as a radial excitation of η'. We find*

$$\frac{\Gamma(\text{J}/\psi\to\gamma+\iota)}{\Gamma(\text{J}/\psi\to\gamma+\eta')}=\frac{x_\iota}{x_{\eta'}}\left|\frac{H_{\text{PS}}(x_\iota)}{H_{\text{PS}}(x_{\eta'})}\right|^2\frac{m_\iota}{m_{\eta'}}\frac{R_\iota^2/m_\iota^2}{R_{\eta'}^2/m_{\eta'}^2}=1.41\,\frac{R_\iota^2/m_\iota^2}{R_{\eta'}^2/m_{\eta'}^2}\,. \tag{4.5}$$

For pseudoscalar mesons there is no empirical information on the wave function of radial excitations. For vector mesons the following regularity is observed:

$$\frac{\Gamma(\Upsilon'\to e^+e^-)}{\Gamma(\Upsilon\to e^+e^-)}\approx\frac{\Gamma(\psi'\to e^+e^-)}{\Gamma(\psi\to e^+e^-)}\approx0.46\,, \tag{4.6}$$

and for ϕ'/ϕ and ρ'/ρ the corresponding ratio seems to be even larger (0.54 ± 0.1

* If we incorporate the mass dependence of α_s, this estimate is lowered by a factor 0.5.

and 1.1 ± 0.2)*. If we use $(R_\iota^2 m_{\eta'}^2 / R_{\eta'}^2 m_\iota^2) = 0.54$ as suggested from ϕ'/ϕ we find

$$\frac{\Gamma(J/\psi \to \gamma + \iota)}{\Gamma(J/\psi \to \gamma + \eta')} = 0.76\,, \tag{4.7}$$

in reasonable agreement with experiment.**

Taking the absolute normalizations as before, an interesting pattern is predicted for the radiative decay of ψ'. The ratio of the branching ratios is given by

$$\frac{\mathrm{Br}(\psi' \to \gamma + 0^-)}{\mathrm{Br}(\psi \to \gamma + 0^-)} = \frac{\mathrm{Br}(\psi' \to e^+e^-)}{\mathrm{Br}(\psi \to e^+e^-)} \left(\frac{M_\psi}{M_{\psi'}}\right)^2 \frac{(1 - m^2/M_{\psi'}^2)}{(1 - m^2/M_\psi^2)} \left|\frac{H(m^2/M_{\psi'}^2)}{H(m^2/M_\psi^2)}\right|^2$$

$$= 0.13 \cdot \begin{Bmatrix} 0.70 \text{ for } \eta \\ 0.72 \text{ for } \eta' \\ 0.78 \text{ for } \iota \end{Bmatrix}, \tag{4.8}$$

consistent with the expectations from quark counting rules [24]. Thus our model explains why this ratio is found to be below the naive expectation of 0.13.

A crucial test, which will allow us to discriminate our approach from other models, will be the radiative decay of Υ. Models based on the duality between the two gluon P-wave amplitude and η' production [2] or on QCD sum rules*** predict a strong decrease of η' production with increasing quarkonium mass $\sim M^{-6}$, since the emission of a pair of quasireal gluons in the 0^{-+} state is strongly suppressed. This is reflected in our calculation in the strong decrease of the absorbtive part. However, for the total rate, which is dominated by the dispersive part, we find a behaviour roughly $\sim M^{-2}$. The analogue of eq. (4.8) then yields

$$\frac{\mathrm{Br}(\Upsilon \to \gamma + 0^-)}{\mathrm{Br}(J/\psi \to \gamma + 0^-)} = \frac{\mathrm{Br}(\Upsilon \to \mu^+\mu^-)}{\mathrm{Br}(J/\psi \to \mu^+\mu^-)} \times \begin{Bmatrix} 0.10 \text{ for } \eta \\ 0.10 \text{ for } \eta' \\ 0.12 \text{ for } \iota \end{Bmatrix}. \tag{4.9}$$

If we allow α_s to decrease from J/ψ to Υ, these predictions could be lowered by a factor ~ 2. We thus predict $\mathrm{Br}(\Upsilon \to \gamma + \eta') \sim 2 \cdot 10^{-4}$, a rate eventually accessible to experiment.

The decays of Υ into a photon and charmonium are theoretically of great interest since in this case all our approximations are well founded. The corresponding branching ratios, however, are rather tiny, typically around 10^{-5}. They are listed in table 5. In this case the purely electromagnetic contribution is no longer negligible, and has to be added coherently. For example, in the $\Upsilon \to \gamma + \eta_c$ case it interferes constructively and rises the branching ratio by a factor 2 [4]. We shall not list the corresponding contributions to P-wave production, since they are extremely small.

* The following leptonic widths have been quoted [14]: $\Gamma(\phi' \to e^+e^-) = 0.69 \pm 0.11$ keV; $\Gamma(\rho' \to e^+e^-) = 7.5 \pm 1.5$ keV.

** Even if we take the mass dependence of α_s into account, there is no striking disagreement considering the large theoretical and experimental uncertainties.

*** Compare the discussion of ref. [15], following eq. (12).

(*b*) *Tensor mesons.* Among the various P-states only the f meson has been seen clearly in radiative J/ψ decays. We obtain the derivative of the radial wave function at the origin ($R'^2_f(0) = 7.7 \cdot 10^{-3}$ GeV^5) through the non-relativistic formula for the two-photon decay

$$\Gamma(f \to \gamma\gamma) = \tfrac{576}{5}\alpha^2 \langle Q^2 \rangle^2 |R'_P(0)|^2 / m^4 , \tag{4.10}$$

derived from eq. (2.3) with the experimental input $\Gamma(f \to \gamma\gamma) \simeq 3$ keV [16] and $\langle Q^2 \rangle = 0.41$ from eq. (4.2) ($\theta_T = 26°$). We multiply eq. (2.25) by $3 \cos^2 \theta_T$, use $\alpha_s = 0.275$, as suggested by eq. (4.3) and find $\Gamma(J/\psi \to \gamma + f) = 88$ eV in excellent agreement with the data.

To estimate f′ production, we use SU(3) since the two photon widths are not well known to date. To wit, we equate (R'^2/m^4) and find*

$$\mathrm{Br}\,(J/\psi \to \gamma + f') = \mathrm{Br}\,(J/\psi \to \gamma + f)\left(\frac{\alpha_s(f')}{\alpha_s(f)}\right)^4 \frac{x_{f'}|H(x_{f'})|^2}{x_f|H(x_f)|^2}\frac{m_{f'}}{m_f}\tan^2\theta_T = 0.37 \cdot 10^{-3} \tag{4.11}$$

in nice agreement with the recent experimental result [22] of $(3.2 \pm 1.0 \pm 1.6) \cdot 10^{-4}$. Very little is known about the wave function of radially excited P-states. To get an idea about the potential order of magnitude, we reduce $R'^2(0)/m^4$ by a factor 0.5 in an ad hoc manner. For an SU(3) scalar state of mass 1640 MeV we then find a branching ratio of around 10^{-3}, a number compatible with our present knowledge on J/$\psi \to \gamma + \theta(1640)$.

The corresponding branching ratios for ψ' and Υ decays are listed in table 4, those for $\Upsilon \to \gamma + \chi_J$ in table 5. Measurements of all Υ modes are difficult but experimentally challenging.

(*c*) *Axial vector mesons.* For a while the reaction J/$\psi \to \gamma + \iota(1440)$ was misinterpreted as J/$\psi \to \gamma$ + E(1420) and the relatively large rate for the decay into the axial vector meson was considered as a great surprise. By now it is well known that the ι should be interpreted as pseudoscalar [15]. Nevertheless, a sizeable contribution from E could be hiding underneath the ι. Experiments have looked for D(1285)

TABLE 3

Predictions of our model for the branching ratios of radiative J/ψ decays

X	η'	$0^{++}(1300)$, SU(3) singlet	D	E	f	f′
Br (J/$\psi \to \gamma$ + X) $\cdot 10^3$	3.0	1.6	1.0	0.4	1.5	0.4

For η see discussion in the main text. Our input values are $|R_\psi(0)|^2 = 0.46$ GeV^3, $|R_{\eta'}(0)|^2 = 0.059$ GeV^3; $|R'_p(0)|^2/m^4 = 2.96 \cdot 10^{-3}$ GeV for all P-waves and α_s^4 from eq. (4.3).

* Alternatively we could have related also R'^2 or R'^2/m^5. The resulting uncertainty is a factor between 0.5 and 1.2.

TABLE 4

Predictions of our model for the branching ratios of radiative ψ' and Y decays $r(V,X) \equiv \mathrm{Br}(V \to \gamma X)/\mathrm{Br}(J/\psi \to \gamma X)\,\mathrm{Br}(J/\psi \to \mu^+\mu^-)/\mathrm{Br}(V \to \mu^+\mu^-)$

X	η	η'	ι	$0^{++}(1300)$	D	E	f	f'
$r(\psi', X)$	0.70	0.73	0.78	0.67	0.76	0.75	0.76	0.74
$r(Y, X)$	0.10	0.11	0.13	0.24	0.15	0.16	0.24	0.21

and an upper limit of $0.6 \cdot 10^{-3}$ has been quoted [18]. Assuming ideal mixing, i.e. $E = s\bar{s}$, $D = (u\bar{u} + d\bar{d})/\sqrt{2}$, and R'^2/m^4 to be the same for f, D and E, we find

$$\Gamma\left(J/\psi \to \gamma + \begin{Bmatrix} D \\ E \end{Bmatrix}\right) = \begin{Bmatrix} 60 \\ 26 \end{Bmatrix} \mathrm{eV} \triangleq \mathrm{Br}\left(J/\psi \to \gamma + \begin{Bmatrix} D \\ E \end{Bmatrix}\right) = \begin{Bmatrix} 1.0 \\ 0.4 \end{Bmatrix} \cdot 10^{-3}. \quad (4.12)$$

The theoretical branching ratio for D(1285) exceeds the present upper limit of $0.6 \cdot 10^{-3}$. Our model predictions are of course uncertain within a factor ~ 2, if we consider the large uncertainties in the choice of wave function and α_s. Thus we are not worried by this discrepancy; nevertheless, we predict a branching ratio not much below the present upper bound. Branching ratios for ψ' and Y decays again are listed in tables 4 and 5.

(*d*) *Scalar mesons.* Not much is known at present about the wave function and the mixing angle of scalar mesons. For the purpose of illustration we have calculated the radiative width into a SU(3) singlet state of 1300 MeV with the same assumptions as before. We find a branching ratio of $1.6 \cdot 10^{-3}$ which indicates that the $\pi\pi$ signal from a broad 0^{++} resonance in the 1–1.5 GeV region might be a non-negligible background and could eventually even affect the helicity analysis of the $J/\psi \to \gamma + f$ mode.

5. Summary and conclusions

We have calculated amplitudes and rates of radiative $^3S_1(Q\bar{Q})$ decays into $^1S_0(q\bar{q})$ and $^3P_J(q\bar{q})$ mesons. Our model is based on lowest-order perturbative QCD and the non-relativistic and weak-binding approximation for the mesons. Considering

TABLE 5

Radiative Y decays into charmonium (QCD contribution)

	η_c	χ_0	χ_1	χ_2
$\dfrac{\Gamma(Y \to \gamma X)}{\Gamma(Y \to e^+e^-)}$	$12.8 \cdot 10^{-4}$	$3.3 \cdot 10^{-4}$	$3.5 \cdot 10^{-4}$	$4.0 \cdot 10^{-4}$

Our input values are $R_{PS}^2 = 0.98\,\mathrm{GeV}^3$, $R_\chi'^2/m^4 = 1.75 \cdot 10^{-3}\,\mathrm{GeV}$, $\alpha_s = 0.2$. They are obtained from ref. [17] using $\Gamma_{\eta_c} = \frac{8}{3}\alpha_s^2 R_{PS}^2/m^4$ and $\Gamma_{\chi_2} = \frac{128}{5}\alpha_s^2 R_\chi'^2/m^4$.

these approximations our results are in good agreement with the experimentally measured rates. A number of predictions are made for the yet unobserved decays into other P-wave mesons (f', D, E, ε) and for ψ' and Y decays which are well compatible with present upper limits. We do not find a strong suppression of scalar and pseudoscalar channels which would be expected from the duality between "real gluon" emission and meson decay. Our result for the relative magnitude of the three helicity amplitudes of the f meson is at variance with present experiments. However, no provision was made in these analyses for complex amplitudes and a coherent 0^{++} contribution. Radiative decays of Y will provide the most stringent test of our model. For the most prominent channels (η', ι, f) we predict branching ratios of the order $(0.5\text{–}2) \cdot 10^{-4}$. A measurement of these decays should constitute an important aim of future experiments at CESR and DORIS.

Part of this work was done while J.G.K. and J.H.K. were visitors at the DESY Theory Group. We would like to thank T. Walsh for hospitality and DESY for support.

Appendix A

COVARIANT HELICITY PROJECTORS

As has been explained in the main text, it is convenient to convert loop integrands involving loop momentum tensors into scalar integrands by contractions with outer momenta. Integrand scalars involving loop momenta can then by partially cancelled against pole denominators thus reducing the number of necessary Feynman parameter integrations. In this appendix we develop a systematic approach to the necessary contractions on the tensor integrands by defining covariant helicity projectors. That is, we expand the transition amplitude along a set of orthogonal covariants for which we choose for convenience a set of helicity covariants. These can be constructed by inverting the matrix that connects the helicity amplitudes to a given set of invariant amplitudes.

We discuss the four cases treated in the main text in turn (K, k, P denote the momenta of 1^{--}, the photon and the decay meson):

(i) $$1^{--}(\alpha) \to \gamma(\nu) + 0^{++}.$$

The transition amplitude $T_{\alpha\nu}$ resulting from the loop integration $T_{\alpha\nu} = \int d^4q\, I_{\alpha\nu}(P, k, q)$ (q = loop momentum) is expressed in terms of the one independent helicity amplitude: $H = H_{s_z(\psi)=1;\, \lambda_\gamma=-1, \lambda_M=0}$ ($H_{-;+0} = H_{+;-0} \equiv H$ from parity)*

$$T_{\alpha\nu} E^\alpha \varepsilon^{*\nu} = H h_{\alpha\nu} E^\alpha \varepsilon^{*\nu}, \tag{A.1}$$

* The positive z-axis is chosen along the momentum of the outgoing meson. We use the Jacob–Wick convention.

where

$$h_{\alpha\nu} = \left(-g_{\alpha\nu} + \frac{k_\alpha P_\nu}{P \cdot k}\right), \tag{A.2}$$

E_α and ε_ν are the polarization vectors of the J/ψ and the photon.

Multiplying (A.1) with $E^{*\alpha'}$ and $\varepsilon^{\nu'}$, doing the spin sums and contracting with $h_{\alpha'\nu'}$ one obtains from (A.1)

$$\begin{aligned} H &= -\tfrac{1}{2} h_{\alpha'\nu'} S^{(1)\alpha\alpha'}(K) g^{\nu\nu'} T_{\alpha\nu} \\ &\equiv \mathbb{P}^{\alpha\nu} T_{\alpha\nu}, \end{aligned} \tag{A.3}$$

where the normalized tensor $\mathbb{P}_{\alpha\nu}(\mathbb{P}^{\alpha\nu}\mathbb{P}^*_{\alpha\nu} = \frac{1}{2})$ will be referred to as a helicity projector. $S^{(1)}_{\alpha\alpha'}(K) = (-g_{\alpha\alpha'} + K_\alpha K_{\alpha'}/M^2)$ is the spin-1 projector of the J/ψ projecting out the appropriate 3-dimensional subspace of a massive spin-1 object. For the photon we have exploited the gauge freedom to write the spin sum as $(-g_{\mu\nu})$.

(ii) $$1^{--}(\alpha) \to \gamma(\nu) + 1^{++}(a)\,.$$

There are two independent helicity amplitudes H_i $(i = 0, 1)$ which we label by the helicity of the 1^{++} meson. From parity one has $H_{-;+0} = H_{+;-0} \equiv H_0$ and $H_{0;++} = H_{0;--} \equiv H_1$. The transition amplitude $T_{\alpha\nu a}$ is written as

$$T_{\alpha\nu a} E^\alpha \varepsilon^{*\nu} e^{*a} = \left(\sum_{i=0,1} H_i h^i_{\alpha\nu a}\right) E^\alpha \varepsilon^{*\nu} e^{*a}, \tag{A.4}$$

where

$$h^0_{\alpha\nu a} = i \frac{m}{(Pk)^2} \varepsilon_{\alpha\nu bc} P^b k^c k_a, \tag{A.5}$$

$$h^1_{\alpha\nu a} = -i \frac{M}{(Pk)^2} k_\alpha \varepsilon_{\nu abc} P^b k^c, \tag{A.6}$$

and where e_a denotes the polarization vector of the 1^{++} meson. Proceeding as before we find for the two helicity projectors

$$\mathbb{P}^{\alpha\nu a}_{(i)} = -\tfrac{1}{2} h^i_{\alpha'\nu'a'} S^{(1)\alpha\alpha'}(K) S^{(1)aa'}(P) g^{\nu\nu'}, \tag{A.7}$$

with $\mathbb{P}_{(i)\alpha\nu a}\mathbb{P}^{*\alpha\nu a}_{(j)} = \frac{1}{2}\delta_{ij}$. The helicity amplitudes are then obtained by the contraction

$$H_i = \mathbb{P}^{*\alpha\nu a}_{(i)} T_{\alpha\nu a}\,. \tag{A.8}$$

(iii) $$1^{--}(\alpha) \to \gamma(\nu) + 2^{++}(ab)\,.$$

There are three independent helicity amplitudes $H_{1;1,0} = H_{1;-1,0} \equiv H_0 H_{0;1,1} = H_{0;-1,-1} \equiv H_1$ and $H_{1;1,2} = H_{-1;-1,-2} \equiv H_2$. We have labelled the helicity amplitudes H_i by the helicity of the 2^{++} meson. The covariant expansion along the helicity amplitudes reads

$$T_{\alpha\nu ab} E^\alpha \varepsilon^{*\nu} e^{*ab} = \left(\sum_{i=0,1,2} H_i h^i_{\alpha\nu ab}\right) E^\alpha \varepsilon^{*\nu} e^{*ab}, \tag{A.9}$$

where

$$h^0_{\alpha\nu ab} = -\tfrac{1}{2}\sqrt{6}\,\frac{m^2}{(P\cdot k)^2}\left(g_{\nu\alpha} - \frac{P_\nu k_\alpha}{P\cdot k}\right)k_a k_b\,, \tag{A.10}$$

$$h^1_{\alpha\nu ab} = \sqrt{2}\,\frac{mM}{(P\cdot k)^2}\left(g_{\nu a} - \frac{P_\nu k_a}{P\cdot k}\right)k_\alpha k_b\,, \tag{A.11}$$

$$\begin{aligned} h^2_{\alpha\nu ab} = &-\frac{1}{P\cdot k}\,g_{a\alpha}(P\cdot k g_{b\nu} - P_\nu k_b) \\ &-\frac{1}{2}\,\frac{(M^2+m^2)}{(P\cdot k)^2}\left(g_{\nu a} - \frac{P_\nu k_a}{P\cdot k}\right)k_\alpha k_b \\ &+\frac{1}{2}\,\frac{m^2}{(P\cdot k)^2}\left(g_{\nu\alpha} - \frac{P_\nu k_\alpha}{P\cdot k}\right)k_a k_b\,. \end{aligned} \tag{A.12}$$

The helicity projectors are given by

$$\mathbb{P}^{\alpha\nu ab}_{(i)} = -\tfrac{1}{2}h^i_{\alpha'\nu'a'b'}S^{(1)\alpha\alpha'}(K)S^{(2)aba'b'}(P)g^{\nu\nu'}\,, \tag{A.13}$$

with $\mathbb{P}^{\alpha\nu ab}_{(i)}\mathbb{P}^*_{(j)\alpha\nu ab} = \tfrac{1}{2}\delta_{ij}$. $S^{(2)}_{aba'b'}$ is the spin-2 projector

$$S^{(2)}_{aba'b'} = \tfrac{1}{2}(S^{(1)}_{aa'}S^{(1)}_{bb'} + S^{(1)}_{ab'}S^{(1)}_{ba'}) - \tfrac{1}{3}S^{(1)}_{ab}S^{(1)}_{a'b'}\,.$$

The helicity amplitudes are then obtained by the contraction

$$H_i = \mathbb{P}^{*\alpha\nu ab}_{(i)}T_{\alpha\nu ab}\,. \tag{A.14}$$

(iv) $$1^{--}(\alpha)\to\gamma(\nu)+0^{-+}\,.$$

In this case there is only one independent helicity amplitude $H = H_{1;-1,0} = -H_{-1;1,0}$. The covariant expansion of the transition amplitude reads

$$T_{\alpha\nu}E^\alpha\varepsilon^{*\nu} = Hh_{\alpha\nu}E^\alpha\varepsilon^{*\nu}\,, \tag{A.15}$$

where

$$h_{\alpha\nu} = i\,\frac{1}{P\cdot k}\,\varepsilon_{\alpha\nu cd}P^c k^d\,. \tag{A.16}$$

The helicity projector is quite simple in this case due to the fact that only the metric contraction of the spin-1 projector survives. One has

$$\begin{aligned} &\mathbb{P}^{\alpha\nu}\mathbb{P}^*_{\alpha\nu} = \tfrac{1}{2}\,, \\ &\mathbb{P}^{\alpha\nu} = -\tfrac{1}{2}h_{\alpha'\nu'}S^{(1)\alpha\alpha'}(K)g^{\nu\nu'} = -\tfrac{1}{2}h^{\alpha\nu}\,, \end{aligned} \tag{A.17}$$

and, finally,

$$H = \mathbb{P}^{*\alpha\nu}T_{\alpha\nu}\,. \tag{A.18}$$

Appendix B

MULTIPOLE AMPLITUDES

The multipole expansion of the transition amplitude is very useful in the limit $m^2/M^2 \to 1$, i.e. when the photon is soft. One expects on very general grounds that the lowest multipole contribution dominates the transition in this limit. We have used this as a consistency check on our calculations in the main text.

For the cases $1^{--} \to \gamma + 0^{++}(0^{-+})$ there is only one multipole each, namely the electric E1 and magnetic M1 dipole transition, respectively. In the case $1^{--} \to \gamma + 1^{++}$ one has the electric dipole (E1) and magnetic quadrupole (M2) transitions. From ref. [23] one finds

$$\mathrm{E1} = \sqrt{\tfrac{1}{2}}\,(H_0 + H_1)\,, \qquad \mathrm{M2} = \sqrt{\tfrac{1}{2}}\,(H_0 - H_1)\,. \tag{B.1}$$

For the case $1^{--} \to \gamma + 2^{++}$ there is in addition to the E1 and M2 transitions the electric octupole transition E3. One has

$$\begin{aligned}
\mathrm{E1} &= \sqrt{\tfrac{1}{10}}\,(-H_0 - \sqrt{3}\,H_1 - \sqrt{6}\,H_2)\,,\\
\mathrm{M2} &= \sqrt{\tfrac{1}{6}}\,(-\sqrt{3}H_0 - H_1 + \sqrt{2}\,H_2)\,,\\
\mathrm{E3} &= \sqrt{\tfrac{1}{15}}\,(-\sqrt{6}\,H_0 + \sqrt{8}\,H_1 - H_2)\,,\\
\mathrm{H}_0 &= \sqrt{\tfrac{1}{10}}\,(-\mathrm{E1} - \sqrt{5}\,\mathrm{M2} - 2\mathrm{E3})\,,\\
\mathrm{H}_1 &= \sqrt{\tfrac{1}{30}}\,(-3\mathrm{E1} - \sqrt{5}\,\mathrm{M2} + 4\mathrm{E3})\,,\\
\mathrm{H}_2 &= \sqrt{\tfrac{1}{15}}\,(-3\mathrm{E1} + \sqrt{5}\,\mathrm{M2} - \mathrm{E3})\,.
\end{aligned} \tag{B.2}$$

Appendix C

ALGEBRAIC IDENTITIES FOR P-WAVE NUMERATORS AND RESULTS FOR LOOP INTEGRALS

In the evaluation of P-wave helicity amplitudes we encounter integrals of the type

$$I = \frac{i}{\pi^2}\int \tfrac{1}{16}\,\mathrm{d}^4 q f(q, k, P)[Q_1 Q_2 G_1 G_2 B^2]^{-1}\,,$$

$$q = k_1 - k_2\,, \qquad P = k_1 + k_2, \tag{C.1}$$

where f denotes a scalar even polynomial of fourth order in q and

$$\begin{aligned}
G_{1,2} &\equiv k_{1,2}^2 + i\varepsilon = \tfrac{1}{4}(q^2 \pm 2q\cdot P + m^2 + i\varepsilon)\,,\\
Q_{1,2} &\equiv -(k + k_{2,1})\cdot k_{1,2} = \tfrac{1}{4}(q^2 \pm 2q\cdot k - M^2)\,,\\
B &\equiv -k_1 \cdot k_2 = \tfrac{1}{4}(q^2 - m^2)\,.
\end{aligned} \tag{C.2}$$

The following identities will be useful:

$$q\cdot P = G_1 - G_2\,, \qquad q\cdot k = Q_1 - Q_2\,,$$
$$1 = (G_1+G_2-2B)/m^2\,,$$
$$1 = 2(Q_1+Q_2-2B)/(m^2-M^2)\,,$$
$$1 = 2(G_1+G_2-Q_1-Q_2)/(m^2+M^2)\,. \tag{C.3}$$

We shall now demonstrate that the integrand can be decomposed into a sum of three-point functions through the help of the following successive sequence of substitutions which have been performed with the help of Schoonschip for all integrands:

$$q^2 \Rightarrow (4B+m^2)\,, \qquad q^4 \Rightarrow (4B+m^2)^2\,. \tag{C.4}$$

(i) Fourth order in q without B:

$$(qP)^4 \Rightarrow -4N_1+4N_2+(qP)^2m^2(m^2+4B)\,,$$
$$(qk)^4 \Rightarrow -4N_3+4N_4+(qk)^2\left(\frac{m^2-M^2}{2}\right)\left(\frac{m^2-M^2}{2}+4B\right),$$
$$(qP)^3(qk) \Rightarrow -4N_5+4N_6+(qP)(qk)m^2(m^2+4B)\,,$$
$$(qk)^3(qP) \Rightarrow -4N_7+4N_6+(qP)(qk)\left(\frac{m^2-M^2}{2}\right)\left(\frac{m^2-M^2}{2}+4B\right),$$
$$(qk)^2(qP)^2 \Rightarrow -4N_8+4N_4+(qk)^2m^2(m^2+4B)\,. \tag{C.5}$$

(ii) (Second order in q) $*$ B

$$B(qP)^2 \Rightarrow -4N_9+2N_{10}+2B^2m^2+Bm^4\,,$$
$$B(qk)^2 \Rightarrow -4N_{11}+2N_{12}+2B^2\left(\frac{m^2-M^2}{2}\right)+B\left(\frac{m^2-M^2}{2}\right)^2,$$
$$B(qP)(qk) \Rightarrow N_{13}\,. \tag{C.6}$$

(iii) Second order in q without B

$$(qP)^2 \Rightarrow -4N_{14}+4B^2+m^2(m^2+4B)\,,$$
$$(qk)^2 \Rightarrow -4N_{15}+4B^2+\left(\frac{m^2-M^2}{2}\right)\left(\frac{m^2-M^2}{2}+4B\right),$$
$$(qp)(qk) \Rightarrow N_{16}\,. \tag{C.7}$$

(iv) Independent of q and B

$$1 \Rightarrow \frac{2}{m^2(m^2-M^2)} N_{17} + \frac{4}{M^2+m^2}\left(\frac{1}{m^4} - \frac{4}{(m^2-M^2)^2}\right) N_{18} + \frac{8}{M^2+m^2}\left(\frac{4}{(m^2-M^2)^2} N_{10} - \frac{1}{m^4} N_{12}\right). \tag{C.8}$$

(v) (Independent of q) $*$ B

$$B \Rightarrow -\frac{4}{m^2(m^2-M^2)} N_{10} + \frac{2}{m^2(m^2-M^2)} N_{18} - 2\frac{B^2}{m^2}. \tag{C.9}$$

(vi) B^2

$$B^2 \Rightarrow \frac{2}{M^2+m^2}(N_{10} - N_{12}). \tag{C.10}$$

$N_1 - N_{18}$ stand for numerators, which immediately lead to two- or three-point functions:

$$\begin{aligned}
N_1 &\equiv (qP)^2 G_1 G_2, & N_2 &\equiv (qP)(G_1 - G_2)B^2, \\
N_3 &\equiv (qk)^2 Q_1 Q_2, & N_4 &\equiv (qk)(Q_1 - Q_2)B^2, \\
N_5 &\equiv (qP)(qk) G_1 G_2, & N_6 &\equiv (qP)(Q_1 - Q_2)B^2, \\
N_7 &\equiv (qP)(qk) Q_1 Q_2, & N_8 &\equiv (qk)^2 G_1 G_2, \\
N_9 &\equiv G_1 G_2 B, & N_{10} &\equiv (G_1 + G_2)B^2, \\
N_{11} &\equiv Q_1 Q_2 B, & N_{12} &\equiv (Q_1 + Q_2)B^2, \\
N_{13} &\equiv (G_1 - G_2)(Q_1 - Q_2)B, & N_{14} &\equiv G_1 G_2, \\
N_{15} &\equiv Q_1 Q_2, & N_{16} &\equiv (G_1 - G_2)(Q_1 - Q_2), \\
N_{17} &\equiv (G_1 + G_2)(Q_1 + Q_2), & N_{18} &\equiv (G_1 + G_2)(Q_1 + Q_2)B,
\end{aligned} \tag{C.11}$$

The resulting individual integrals are partly infrared divergent, which is an artifact of our decomposition. We introduce an infrared cutoff ε, and, after combining all integrals, all terms proportional to ε^{-1} and $\ln \varepsilon$ cancel as expected. We now list the integrals

$$I_i = \frac{i}{\pi^2} \int \tfrac{1}{16} \mathrm{d}^4 q \, N_i [Q_1 Q_2 G_1 G_2 B^2]^{-1}, \tag{C.12}$$

where apparently at most three denominators survive:

$$I_1 = 4\left[\frac{60 - 96x + 35x^2}{18x^2} + \frac{(10-x)(1-x)^2}{3x^3} \ln(1-x)\right],$$

$$I_2 = 2\left[\frac{2-x}{x}(\mathscr{L}_2(1) - \mathscr{L}_2(1-2x)) - 4 - \frac{2x}{1-2x} \ln(2x)\right],$$

$$I_3 = \frac{2}{3}\left(\frac{x}{1-x}\right)^2 [-4 + \ln 2 - 3\ln\varepsilon - \tfrac{1}{2}i\pi],$$

$$I_4 = 2\Big[\frac{2-x}{x}(\mathscr{L}_2(1-2x) - 2\mathscr{L}_2(1-x) - \tfrac{1}{2}\ln^2(1-x) + \mathscr{L}_2(1))$$
$$- \frac{2x}{1-2x}\ln(2x) - 4\ln 2 - 2\ln(1-x) + i\pi\left(2 + \frac{2-x}{x}\ln(1-x)\right)\Big],$$

$$I_5 = 2\left[\frac{2-x}{x} + 2\frac{1-x}{x^2}\ln(1-x)\right],$$

$$I_6 = -2\frac{2x}{1-2x}\ln(2x),$$

$$I_7 = -4\frac{x}{1-x}[1 + \ln\varepsilon],$$

$$I_8 \equiv 0,$$

$$I_9 = 4\frac{1}{M^2 x}\left[1 + \frac{1-x}{x}\ln(1-x)\right],$$

$$I_{10} = 4\frac{1}{M^2 x}[\mathscr{L}_2(1) - \mathscr{L}_2(1-2x)],$$

$$I_{11} = -4\frac{1}{M^2(1-x)}[\ln 2 - \tfrac{1}{2}i\pi],$$

$$I_{12} = -4\frac{1}{M^2 x}[\mathscr{L}_2(1-2x) - 2\mathscr{L}_2(1-x) - \tfrac{1}{2}\ln^2(1-x)$$
$$+ \mathscr{L}_2(1) + i\pi\ln(1-x)],$$

$$I_{13} = 8\frac{1}{M^2 x}[\mathscr{L}_2(1-x) - \mathscr{L}_2(1-2x) - \ln 2\ln(1-x)$$
$$- \ln\varepsilon\ln(1-x)],$$

$$I_{14} = \left(\frac{4}{M^2 x}\right)^2\left[2 + \frac{2-x}{x}\ln(1-x)\right],$$

$$I_{15} = 8\left(\frac{1}{M^2(1-x)}\right)^2[\ln 2 - \ln\varepsilon - \tfrac{1}{2}i\pi],$$

$$I_{16} = \left(\frac{4}{M^2 x}\right)^2\left[\left(\frac{2x}{1-x} + 2\ln(1-x)\right)\left(\frac{1}{\varepsilon} - 1\right)\right.$$
$$\left. + \frac{x}{1-x}\ln\varepsilon - \frac{x}{1-x}\ln(2x) - \ln(1-x)\right],$$

$$I_{17} = -\left(\frac{4}{M^2 x}\right)^2 \left[\frac{x}{1-x}\ln(2x) + \ln(1-x) - \frac{x}{1-x}\ln\varepsilon + \left(\frac{2x}{1-x} + 2\ln(1-x)\right)\left(\frac{1}{\varepsilon} - 1\right)\right],$$

$$I_{18} = 8\frac{1}{M^2 x}[\mathscr{L}_2(1-x) - \mathscr{L}_2(1-2x) - \ln 2 \ln(1-x) + \ln\varepsilon \ln(1-x)]. \qquad \text{(C.13)}$$

The Spence function $\mathscr{L}_2(x)$ is defined as

$$\mathscr{L}_2(x) = -\int_0^x \frac{\ln(1-t)}{t} \mathrm{d}t.$$

References

[1] A. Ore and J.L. Powell, Phys. Rev. 75 (1949) 1696;
M. Chanowitz, Phys. Rev. D12 (1975) 918;
K. Koller and T.F. Walsh, Phys. Lett. 72B (1977) 227; (E: 73B (1978) 504;
S. Brodsky, T.A. DeGrand, R.R. Horgan and D.G. Coyne, Phys. Lett. B73 (1978) 203;
H. Fritzsch and K.H. Streng, Phys. Lett. 74B (1978) 9
[2] A. Billoire, R. Lacaze, A. Morel and H. Navalet, Phys. Lett. 80B (1979) 381;
R. Lacaze and H. Navalet, Nucl. Phys. 80B (1979) 381
[3] M. Krammer, Phys. Lett. 74B (1978) 361
[4] B. Guberina and J.H. Kühn, Nuovo Cim. Lett. 32 (1981) 295;
J.H. Kühn, Proc. Workshop on Doris experiments, DESY, 10–11 February 1981
[5] T. Munehisa, Progr. Theor. Phys. 63 (1980) 734
[6] A. Devoto and W.W. Repko, Phys. Lett. 106B (1981) 501
[7] J. Körner and M. Krammer, Z. phys. C16 (1983) 279
[8] J. Körner, J.H. Kühn and H. Schneider, Phys. Lett. 120B (1983) 444
[9] A. Nishimura, Glasgow preprint 1979
[10] J.H. Kühn, J. Kaplan and E.G.O. Safiani, Nucl. Phys. 157B (1979) 125
[11] P.K. Kabir and A.J. Hey, Phys. Rev. D13 (1976) 3161
[12] G. Alexander et al., Phys. Lett. 76B (1978) 652
[13] W. Bartel et al., DESY 82-007 (1982);
G.S. Abrams et al., Phys. Rev. Lett. 43 (1979) 477;
H.J. Behrend et al., Nucl. Phys. B211 (1983) 369
[14] B. Delcourt, Proc. 1981 Int. Symp. on lepton and photon interactions, Bonn
[15] V. Novikov, M. Shifman, A. Vainshtein and V. Zakharov, Nucl. Phys. B165 (1980) 55
[16] R.J. Wedemeyer, Proc. 1981 Int. Symp. on lepton and photon interactions, Bonn
[17] D.L. Scharre, Proc. 1981 Int. Symp. on lepton and photon interactions, Bonn
[18] Review of particle properties, April 1982, Phys. Lett. 111B (1982)
[19] MARK II, G. Feldmann, Les Arcs 1980 Proc.
[20] DASP, W. Fues, thesis, MPI-preprint PAE/Exp, E1. 92 (1981)
[21] D.L. Scharre, Proc. 20th Int. Conf. on high energy physics, Madison
[22] E. Bloom, talk presented at the 20th Int. Conf. high energy physics, Paris 1982
[23] W.N. Cottingham and B.R. Pollard, Ann. of Phys. 105 (1977) 111
[24] S. Brodsky and P. Lapage, Phys. Rev. D24 (1981) 2848
[25] J.H. Kühn, Phys. Lett. 127B (1983) 257